



PLANAR MOTION OF AN ARTICULATED TOWER WITH AN ELASTIC APPENDAGE

P. BAR-AVI AND H. BENAROYA

*Department of Mechanical and Aerospace Engineering, Rutgers University, Piscataway,
NJ 08855, U.S.A.*

(Received 17 November 1995 and in final form 8 April 1996)

Masts, antennas and other appendaged towers connected to offshore platforms are subjected to harsh environmental conditions. In this paper, the dynamic response of such a structure is investigated. The mast is assumed to be fixed at bottom to an articulated tower and carrying a concentrated mass at the other end. The mast is modelled as a continuous system (beam-like), subjected to wind forces. The equation of motion formulated in this paper is general enough to represent a partially submerged articulated tower or an appendaged tower. In the derivation of the equation of motion, non-linearities due to large lateral displacements as well as rotation, drag wind and wave forces, which are assumed to be proportional to the square relative velocity between the wind/wave and the mast, are considered. The motion of the articulated tower, to which the mast is connected, is also included in the dynamics as a base excitation. The non-linear partial differential equation of motion is then non-dimensionalized and simplified to show that the rotation (inertia) term is negligible. The equation of motion is numerically solved using finite difference approximations, which are embedded in the commercial code “ACSL” (Advanced Continuous Simulation Language). The response of the mast to deterministic and random wind and wave is investigated and some parameter studies are conducted. Bending and shear stresses are calculated for different environmental conditions. The model was also used to verify the rigid body assumption frequently used in analyzing the response of a partially submerged articulated tower.

© 1996 Academic Press Limited

1. INTRODUCTION

Compliant platforms such as articulated towers are economically attractive for deep water conditions because of their reduced structural weight compared to conventional platforms. The foundation of the tower does not resist lateral forces due to wind, waves and currents; instead, restoring moments are provided by a large buoyancy force, a set of guylines or a combination of both. These structures have a fundamental frequency well below the wave lower-bound frequency. As a result of the relatively large displacements, geometric non-linearity is an important consideration in the analysis of such a structure. Most investigators have considered the tower to be an upright rigid pendulum attached to the sea floor via a pivot having one or two degrees of freedom. Single-degree-of-freedom models were investigated by Bar-Avi and Benaroya [1], Chakrabarti and Cotter [2], Gottlieb *et al.* [3], Muhuri [4] and Datta and Jain [5–7]. Two-degree-of-freedom models were studied by Bar-Avi and Benaroya [8, 9], Kirk and Jain [10, 11], Olsen *et al.* [12] and Chakrabarti and Cotter [13]. A detailed description of these studies and others is given in reference [14]. None of these papers verified the validity of the rigid body assumption, one of the tasks of this paper.

Flexible articulated towers have also been considered. In two papers, by Havery *et al.* [15] and by McNamara and Lane [16], a finite element method is used to calculate the response of a planar flexible multi-articulated tower. Examples of the response of single point moorings, bi-articulated and multi-articulated towers were presented.

The objective of the paper by Leonard and Young [17] was to develop a solution method to evaluate the dynamic response of an articulated tower. The method is based on three-dimensional finite elements. The tower was subjected to waves and currents, and geometric and drag force non-linearities were included. The response was evaluated numerically for steady current only and then for waves.

Sebastiani *et al.* [18] presented the design and dynamic analysis of a 1000 m single point mooring tower in the Mediterranean Sea. The tower consists of four slender columns, about 3 m in diameter, connected via a universal joint. A buoyancy chamber is welded to the upper columns, just underneath the deck. The tower is so flexible that several natural frequencies are within the range of the wave frequency: therefore, it operates under resonance conditions. The structure was modelled using finite elements, and forces due to waves, currents and wind were considered. In the dynamic analysis that was performed for survival and station-keeping conditions, irregular seas characterized by the Pierson–Moskowitz spectrum were considered. To gain a better understanding of the dynamic behavior, a model test program was launched. A model having a scale of 1:107.5 was built and tested. The tests were performed for the structure alone in wind, currents and waves, and then with a tanker moored to the structure. The test results showed reasonable agreement with simulations for the maximum forces. As for the dynamic behavior, the theoretical predictions did not agree with the tests. A detailed description of these and other studies is provided in Adrezin *et al.* [14].

In all analyses performed on flexible articulated towers, the finite element approach has been used. In this paper, which presents a study of the non-linear dynamic response of a flexible appendage or articulated tower, the dynamics of the continuous system are used. First, the non-linear partial differential equation of motion is derived, including non-linearities due to geometry, drag force, added mass, buoyancy, wind and base excitation. All forces are evaluated at the instantaneous position of the tower and, therefore, they are not only time-dependent but also highly non-linear. The equation is then solved for two cases; a partially submerged articulated tower and an appendaged tower connected to the deck of an articulated offshore tower. The numerical solution was obtained using finite difference approximations embedded in “ACSL” software and typical behavior was identified.

2. PROBLEM DESCRIPTION

The derivation and analysis of a beam-like structural model, presented in this paper, is motivated by two main objectives: (1) proving the validity of the rigid body assumption for the articulated tower that was investigated in the paper by Bar-Avi and Benaroya [1]; and (2) to expand the model to include an appendaged tower, i.e., an antenna or mast, connected to the deck of the articulated tower.

The schematic of the model considered is shown in Figure 1. The model consists of a tower partially submerged in the ocean having a concentrated mass at the top. The tower's lateral deflection is $y(x, t)$, and it is subjected to wave, current and wind loads as well as to possible base excitation. All forces/moments, velocities and accelerations are derived and expressed in the fixed co-ordinate system x, y . This model is sufficiently general to represent either the partially submerged articulated tower or an appendage connected to the tower's deck. This is done by changing the boundary conditions and the external forces.

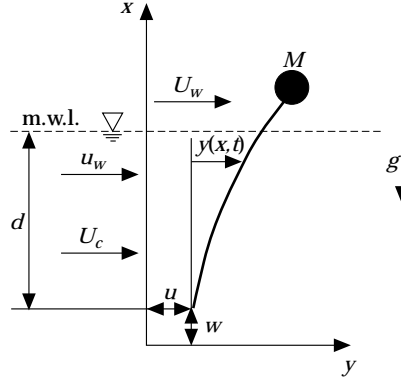


Figure 1. A schematic of the model.

3. EQUATION OF MOTION

The equation of motion is derived under several assumptions: (1) an inextensible beam with planar motion only, $y = y(x, t)$; (2) a flexible tower, having a bending rigidity EI ; (3) lateral and rotational vibrations only (longitudinal vibrations are negligible); (4) a tower length that is much larger than its diameter, *i.e.*, $l \gg d$; (5) a slender and smooth structure with a circular non-constant cross-section; (6) the tower may be subjected to base excitation, wave, current and wind loads; (7) the current and wind velocities propagate in the direction of the wave.

Since the model studied is continuous, Hamilton's principle is used to derive the equation of motion. Hamilton's principle, in the presence of external forces, states [19] that

$$\int_{t_1}^{t_2} \left[\delta \mathcal{L} + \sum \delta q_i F_{q_i} \right] dt = 0, \quad (1)$$

where the Lagrangian \mathcal{L} is defined as

$$\mathcal{L} = E_K - E_P \quad (2)$$

and E_K and E_P are the kinetic and potential energies, respectively. F_{q_i} is the external force in the direction of the generalized co-ordinate q_i . These forces are found using the virtual work concept. In this problem the Lagrangian is $\mathcal{L} = \mathcal{L}(x, y, y_t, y_x, y_{xx}, y_{xt})$, and the only generalized co-ordinate is y ; *i.e.*, $q_i = y$. Therefore, the Euler-Lagrange equation is (see Courant and Hilbert [20], p. 192),

$$\frac{\partial \mathcal{L}}{\partial y} - \frac{\partial}{\partial t} \left(\frac{\partial \mathcal{L}}{\partial y_t} \right) - \frac{\partial}{\partial x} \left(\frac{\partial \mathcal{L}}{\partial y_x} \right) + \frac{\partial^2}{\partial x^2} \left(\frac{\partial \mathcal{L}}{\partial y_{xx}} \right) + \frac{\partial^2}{\partial x \partial t} \left(\frac{\partial \mathcal{L}}{\partial y_{xt}} \right) = Q, \quad (3)$$

where y_t , y_x , y_{xx} and y_{xt} are the partial derivatives of the displacement y with respect to t and/or x , and Q is the sum of the generalized forces.

4. DERIVATION OF THE LAGRANGIAN

To derive the Lagrangian \mathcal{L} , the potential and kinetic energies must be found. In Figure 2 is shown the geometry of an element $d\bar{m}$ in its initial state and in its perturbed

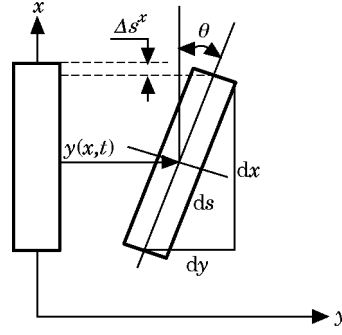


Figure 2. The element geometry.

state, denoted as ds . The element undergoes a lateral displacement $y(x, t)$ and also a rotation $\theta(x, t)$ about the z -axis.

4.1. BENDING STRAIN ENERGY

The expression for the potential strain energy due to bending is given by

$$E_p^b = \int_w^L \frac{1}{128} E \pi D^4(x) \frac{y_{xx}^2}{(1 + y_x^2)^3} \sqrt{1 + y_x^2} dx, \quad (4)$$

where E is Young's modulus and $D(x)$ is the tower diameter. L is the projection of the length of the tower in the x -direction:

$$l = \int_w^L \frac{1}{\cos \theta} dx = \int_w^L \sqrt{1 + y_x^2} dx. \quad (5)$$

4.2. POTENTIAL ENERGY OF APPLIED LOADING

The potential energy due to gravity and buoyancy is given by

$$E_p^{gb} = \int_w^L F_{gb}(x, t) \Delta s^x, \quad (6)$$

where Δs^x is the change in height per unit length, in the x -direction, that the element ds undergoes (see Figure 2):

$$\Delta s^x = \frac{\partial s^x}{\partial x} dx = dx(\sqrt{1 + y_x^2} - 1). \quad (7)$$

The force per unit length $F_{gb}(x, t)$ is due to gravity and buoyancy:

$$F_{gb}(x) = \frac{1}{4} \rho g \pi D^2(x)(l_s - \bar{x} - w) - [\frac{1}{4} \rho_T \pi D^2(x)(w + l - \bar{x}) + M](g + w_{tt}), \quad (8)$$

where ρ_T and ρ are the tower and the fluid densities, respectively, and l is the total length of the tower. The length of the submerged part of the tower, l_s , is determined as

$$l_s = \int_w^d \frac{dx}{\cos \theta} = \int_w^d \sqrt{1 + y_x^2} dx, \quad (9)$$

and \bar{x} is defined as

$$\bar{x} = \int_w^x \frac{dx}{\cos \theta} = \int_w^x \sqrt{1 + y_x^2} dx. \quad (10)$$

Finally, substituting equations (8) and (7) into equation (6) leads to the expression for the potential energy:

$$\begin{aligned} E_p^{gb} &= \int_w^L \frac{1}{4} \rho g \pi D^2(x) (l_s - \bar{x} - w) (\sqrt{1 + y_x^2} - 1) dx \\ &\quad - \int_w^L \left(\frac{1}{4} \rho_T \pi D^2(x) (w + l - \bar{x}) + M \right) (g + w_H) (\sqrt{1 + y_x^2} - 1) dx. \end{aligned} \quad (11)$$

4.3. KINETIC ENERGY

The kinetic energy consists of two components, one due to linear velocity and the other due to angular velocity. It is derived by following a particle $d\bar{m}$ from the non-perturbed system to the perturbed one. The linear velocity kinetic energy is

$$E_K^L = \int_w^L \frac{1}{8} \pi (\rho_T + C_A \rho) D^2(x) [(V^x)^2 + (V^y)^2] dx, \quad (12)$$

where V^x and V^y are the absolute velocities of the tower's element ds in the x -, y -direction. Since the tower's base is not stationary, it is actually a moving continua problem. The absolute velocities in the x -, y -direction are obtained using the procedure described in Bar-Avi and Porat [21] and also Bottega [22]. Hence

$$V^x = \frac{\partial s^x}{\partial t} + w_t \left(1 + \frac{\partial s^x}{\partial x} \right), \quad V^y = \frac{\partial y}{\partial t} + w_t \frac{\partial y}{\partial x} + u_t, \quad (13)$$

where u_t and w_t are the base velocities. Substituting equation (13) into equation (12) results in the expression for the linear kinetic energy expressed in the inertial co-ordinate system x, y :

$$E_K^L = \int_w^L \frac{1}{8} \pi (\rho_T + C_A \rho) D^2(x) \{ (s_t^x + w_t(1 + s_x^x))^2 + (y_t + w_t y_x + u_t)^2 \} dx, \quad (14)$$

where s^x is the position of the element ds in the x -direction.

The angular velocity kinetic energy is

$$E_K^A = \int_w^L \frac{1}{128} \pi (\rho_T + C_A \rho) D^4(x) \frac{y_{xt}^2}{(1 + y_x^2)^2} dx. \quad (15)$$

Thus, the total kinetic energy is

$$E_K = \int_w^L \frac{1}{8}\pi(\rho_T + C_A\rho)D^2(x) \left\{ (s_t^x + w_t(1 + s_x^x))^2 + (y_t + w_t y_x + u_t)^2 + \frac{1}{16}D^2(x) \frac{y_{xt}^2}{(1 + y_x^2)^2} \right\} dx. \quad (16)$$

4.4. THE LAGRANGIAN

Finally, the Lagrangian is found to be

$$\begin{aligned} \mathcal{L} = \int_w^L \left\{ \frac{1}{8}\pi(\rho_T + C_A\rho)D^2(x) \left[(\Delta s_t^x + w_t(1 + \Delta s_x^x))^2 + (y_t + w_t y_x + u_t)^2 \right. \right. \\ \left. \left. + \frac{1}{16}D^2(x) \frac{y_{xt}^2}{(1 + y_x^2)^2} \right] + \frac{1}{128} E\pi D^4(x) \frac{y_{xx}^2}{(1 + y_x^2)^3} \right. \\ \left. - \left[-\frac{1}{4}\rho\pi D^2(x)g(l_s - \bar{x} - w) \right. \right. \\ \left. \left. + \left(\frac{1}{4}\rho_T\pi D^2(x)(g + w_n)(w + l - \bar{x}) + M \right) (\sqrt{1 + y_x^2} - 1) \right] \right\} dx. \quad (17) \end{aligned}$$

5. GENERALIZED FORCES

5.1. GENERAL

The generalized forces are determined using the virtual work concept. Three types of forces are considered in this analysis, all acting in a direction normal to the tower. The first is for the submerged part of the tower, and is due to gravity waves F_{fl} . The second is at the water level and is due to wave slamming F_s , and the third is for the exposed part of the tower, which is above water level and is due to wind load F_w . These forces are shown in Figure 3.

The generalized forces due to external loading are found from

$$Q\delta y = F^n \delta n, \quad (18)$$

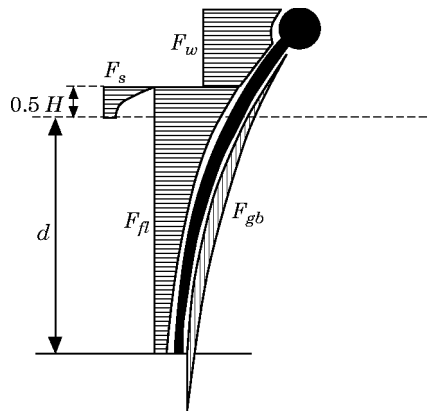


Figure 3. The external forces acting on the tower.

where F^n is any force acting normal to the tower and δn is the tower's displacement in the direction of the force normal to the tower, which is given by

$$\delta n = \delta x \frac{y_x}{\sqrt{1 + y_x^2}}. \quad (19)$$

Thus, we find that

$$Q\delta y = F^n \delta x \frac{y_x}{\sqrt{1 + y_x^2}}. \quad (20)$$

Dividing equation (20) by dx and rearranging leads to the generalized force Q :

$$Q = F^n \frac{1}{\sqrt{1 + y_x^2}}. \quad (21)$$

In the following subsections, the various forces F^n are derived.

5.2. WAVE FORCES

The wave force per unit length due to drag and inertia is approximated via Morison's equation, which states that

$$F_{fl} = \frac{1}{2}C_D\pi\rho D(x)|V_{fl}^n - V_T^n|(V_{fl}^n - V_T^n) + \frac{1}{4}C_M\pi\rho D^2(x)\dot{V}_{fl}^n, \quad (22)$$

where V_{fl}^n and \dot{V}_{fl}^n are the absolute wave velocity and acceleration normal to the tower, respectively, and V_T^n is the tower's velocity in a direction normal to it. Substituting the wave velocities and accelerations as well as the tower velocities into equation (22) leads to the fluid forces. The generalized drag force, Q_D , is then

$$\begin{aligned} Q_D &= C_D\pi\rho D(x) \frac{1}{2(1 + y_x^2)^{3/2}} \\ &\quad \times \left\{ \frac{1}{2}H\omega e^{k(x-d)}(\cos(-ky + \omega t) + y_x \sin(-ky + \omega t)) + U_c - y_t - u_t \right\} \\ &\quad \times \left\{ \frac{1}{2}H\omega e^{k(x-d)}(\cos(-ky + \omega t) + y_x \sin(-ky + \omega t)) + U_c - y_t - u_t \right\}. \end{aligned} \quad (23)$$

Similarly, the inertia force Q_M is given by

$$Q_M = C_M\pi\rho D^2(x) \frac{1}{8}H\omega^2 \frac{e^{k(x-d)}}{(1 + y_x^2)} [-\sin(-ky + \omega t) + y_x \cos(-ky + \omega t)]. \quad (24)$$

5.3. WIND FORCE

The wind force is estimated in a similar way as the drag load. The formulation is the same but the constants are different; see Faltinsen [23]. The wind generalized drag force is given by

$$Q_w = \frac{1}{2}C_{D_a}\rho_a D(x)|U_w^n - y_t - u_t|(U_w^n - y_t - u_t) \frac{1}{(1 + y_x^2)^{3/2}}, \quad (25)$$

where ρ_a is the air density, C_{D_a} is the air drag coefficient, and U_w^n is the wind velocity normal to the tower.

The wind speed U_w^n has two components, one deterministic and the other randomly varying with height above mean water level. The deterministic velocity is related to the constant wind speed at 10 m, U_{10} , and the random velocity is related to the mean gust velocity at 10 m, $(U_{10})_{gust}$, as follows (see Patel [24, p. 186]):

$$U_w = U_{10}(x/10)^{0.113} + (U_{10})_{gust}(x/10)^{0.100}. \quad (26)$$

5.4. DISSIPATIVE FORCE

The dissipative force is assumed to be viscous structural damping; that is,

$$Q_{dis} = Cy_t, \quad (27)$$

where C is the damping coefficient. The velocity used here is due to the tower deflection only, since the structural damping is internal, and hence is not affected by the base excitation.

6. GOVERNING EQUATIONS OF MOTION

The governing equation of motion is derived by setting the dynamic force, i.e., the left side of the Euler–Lagrange equation, equal to the sum of external forces,

$$F_{dyn} = Q_D + Q_M + Q_w - Q_{dis}. \quad (28)$$

The expressions for the dynamic and generalized forces are determined using “MAPLE”. To simplify the Lagrangian, small deformations are assumed, meaning that $ds \simeq dx$, from which it follows that

$$L \simeq l - w, \quad l_s \simeq d - w, \quad \bar{x} \simeq x - w, \quad (29)$$

resulting in $y_x^2 \ll 1$. Since the fully non-linear expressions are very complex, the dynamic force, equation (3), is simplified by a Taylor expansion, neglecting third order and higher terms of the displacement, its derivatives with respect to x and/or t , and products of these derivatives, i.e., y , y_x , y_{xx} , y_{xxx} , y_{xxxx} , y_{xt} and y_{xxt} :

$$\begin{aligned} F_{dyn} = & \frac{1}{64}E\pi D^4 y_{xxxx} + \frac{1}{8}E\pi D^3 D_x y_{xxx} + \left[\frac{1}{16}E\pi D^2 (3D_x^2 + DD_{xx}) + M(g + w_{tt}) \right. \\ & + \frac{1}{4}\pi D^2 (\rho_T + C_A \rho) w_t^2 - \rho g(d - x - w) + \frac{1}{4}\pi D^2 \rho_T (w + l - x)(g + w_{tt}) \left. \right] y_{xx} \\ & - \frac{1}{4}\pi D^3 D_x (\rho_T + C_A \rho) y_{xxt} - \frac{1}{16}\pi D^4 (\rho_T + C_A \rho) y_{xxtt} \\ & + \frac{1}{4}\pi DD_x (\rho_T + C_A \rho) (w_t + 2u_t y_x) (2y_t + 2u_t + 3w_t y_x) \\ & + [D_x (\rho_T (g + w_{tt}) (w + l - x) - \rho g(d - x - w)) - D(\rho_T (g + w_{tt}) - \rho g)] \frac{1}{4}\pi D y_x \\ & + \frac{1}{4}\pi D^2 (\rho_T + C_A \rho) (y_{tt} + 2w_t y_{xt} + u_{tt}). \end{aligned} \quad (30)$$

As mentioned earlier, two general models are considered, (1) the articulated tower alone, and (2) the appendaged tower.

(1) For the articulated tower, all dynamic forces, including the base excitation that can simulate an earthquake, as well as all the external forces have to be considered. The tower is connected to the sea floor via a universal joint and is free at the other end; thus the boundary conditions are as follows:

$$\text{at } x = w, \quad \begin{cases} y = 0, \\ M_b = 0; \end{cases} \quad \text{at } x = L + w, \quad \begin{cases} M_b = 0, \\ M\dot{V}_T = S. \end{cases} \quad (31)$$

The bending moment M_b , the tower’s lateral acceleration \dot{V}_T , and the shear force S , are derived below.

(2) For the appendaged tower, it is assumed that its inertia is much smaller than that of the articulated tower to which it is connected. Hence, the base excitation is taken as the response of the submerged articulated tower. Buoyancy and added mass terms are set

to zero and only wind force is considered. Since the appendaged tower is fixed to the deck and is free at the other end, the following boundary conditions apply:

$$\text{at } x = w, \quad \begin{cases} y = 0, \\ y_x = 0; \end{cases} \quad \text{at } x = L + w, \quad \begin{cases} M_b = 0, \\ M\dot{V}_T = S. \end{cases} \quad (32)$$

The bending moment M_b is

$$M_b = \frac{1}{64}E\pi D^4(x) \frac{y_{xx}}{(1 + y_x^2)^{3/2}}. \quad (33)$$

The tower's lateral acceleration \dot{V}_T is obtained by direct differentiation of equation (13) with respect to time,

$$\dot{V}_T = \frac{\partial V^y}{\partial t} + w_t V_x^y = y_{tt} + 2w_t y_{xt} + w_t^2 y_{xx} + w_{tt} y_x + u_{tt}. \quad (34)$$

The shear force S is determined from Figure 4, which depicts the forces and moments acting on an element ds of the tower. The tower element is in equilibrium, so the shear force S is found from the moment equation about the centroid of the element to be

$$S = \frac{1}{64}E\pi D^4 y_{xxx} - F_{gb} y_x - \frac{1}{16}\pi D^4 (\rho_T + C_A \rho) y_{xtt}. \quad (35)$$

Using the expressions for the bending moment and the shear force along the tower and the small deflection assumption, the axial stress and the shear stress can be evaluated. The axial stress is, due to the bending moment and axial force,

$$\sigma = 32M_b/\pi D^3 - 4F_{gb}/\pi D^2, \quad (36)$$

and the shear stress is

$$\tau = 4S/\pi D^2, \quad (37)$$

where the expressions for M_b , F_{gb} and S were derived earlier. In order to perform

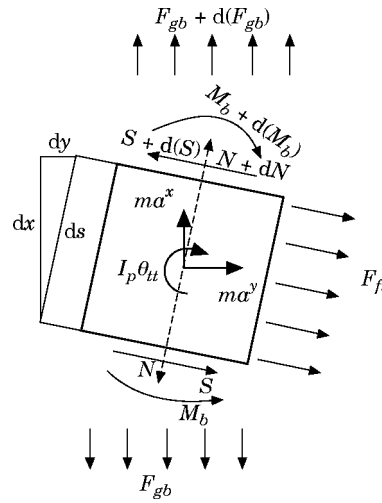


Figure 4. The forces and moments acting on an element.

fatigue or reliability analysis, an equivalent stress can be calculated using the Von Mises formula,

$$\sigma_T = \sqrt{\sigma^2 + 3\tau^2} = \sqrt{(32M_b/\pi D^3 - 4F_{gb}/\pi D^2)^2 + 3(4S/\pi D^2)^2}. \quad (38)$$

7. NUMERICAL SOLUTION

The equation of motion is a non-linear partial differential equation with non-constant coefficients. It is solved numerically using ‘‘ACSL’’. The method of solution is based on the finite difference approach embedded into ‘‘ACSL’’ as shown in a paper by Mitchell and Gauthier [25].

7.1. PARTIALLY SUBMERGED ARTICULATED TOWER

In this section the assumption of rigid body will be shown to be valid for the type of structure that was investigated in the paper by Bar-Avi and Benaroya [1]. The natural frequency and the modes of vibration are the key factors in this proof. It will be shown that the first mode of the system is that of a rigid pendulum and has a much lower frequency and higher amplitude than the second mode, which corresponds to the first elastic mode. The first elastic frequency is also very high compared to the wave excitation frequency, hence not influenced by the wave forces. In order to find an analytical solution for the natural frequencies the following assumptions are made: (1) the buoyancy force acts at the top of the articulated tower; (2) the mass of the deck is much larger than the total mass of the articulated tower, i.e., $M \gg \rho_T \pi (D^2/4)l$; (3) the length of the articulated tower is much larger than its diameter, i.e., $l \gg D$; (4) the cross-section of the articulated tower is constant; (5) there is no base excitation on the articulated tower; (6) rotary inertia is negligible; (7) there are small displacements, i.e., $u/l \ll 1$ about equilibrium position $y = 0$.

Applying the above assumptions in equation of motion (30) yields the following partial differential equation of motion for the articulated tower:

$$y_{xxxx} + Ny_{xx} + \tilde{m}y_{tt} = 0, \quad (39)$$

with boundary conditions

$$\text{at } x = 0 \quad \begin{cases} y = 0, \\ y_{xx} = 0; \end{cases} \quad \text{at } x = l \quad \begin{cases} y_{xx} = 0, \\ y_{xxx} + Ny_x = \tilde{M}y_{tt}, \end{cases} \quad (40)$$

where

$$N = \frac{64g}{E\pi D^4} (M - \frac{1}{4}\rho\pi D^2 d), \quad \tilde{m} = \frac{16g}{ED^2} (\rho_T + C_A\rho), \quad \tilde{M} = \frac{64M}{E\pi D^4}. \quad (41)$$

To solve equation (39), separation of variables with an harmonic solution in time is assumed:

$$y = \bar{y}(x) e^{-i\omega t}. \quad (42)$$

Substituting equation (42) into equation (39) and rearranging terms leads to the equation for the displacement,

$$\bar{y}_{xxxx} + N\bar{y}_{xx} - \tilde{m}\omega^2\bar{y} = 0, \quad (43)$$

with boundary conditions

$$\text{at } x = 0 \quad \begin{cases} \bar{y} = 0, \\ \bar{y}_{xx} = 0; \end{cases} \quad \text{at } x = l \quad \begin{cases} \bar{y} = 0, \\ \bar{y}_{xxx} + N\bar{y}_x + \tilde{M}\omega^2\bar{y} = 0. \end{cases} \quad (44)$$

The solution of equation (43) is

$$\bar{y} = \bar{A} e^{\lambda x}. \quad (45)$$

Substituting equation (45) into equation (43) and rearranging terms leads to the characteristic equation:

$$\lambda^4 + N\lambda^2 - \tilde{m}\omega^2 = 0. \quad (46)$$

Thus, the solution for λ is

$$\begin{aligned} \lambda_{1,2} &= \pm \sqrt{-\frac{1}{2}(N - \beta)} = \pm \sqrt{\frac{1}{2}(\beta - N)} = \pm \alpha_1, \\ \lambda_{3,4} &= \pm \sqrt{-\frac{1}{2}(N + \beta)} = \pm i\sqrt{\frac{1}{2}(\beta + N)} = \pm i\alpha_2, \end{aligned} \quad (47)$$

where

$$\beta = \sqrt{N^2 + 4\tilde{m}\omega^2}. \quad (48)$$

Substituting λ_1 and λ_2 into equation (43) yields

$$\bar{y} = \bar{A} e^{\alpha_1 x} + \bar{B} e^{-\alpha_1 x} + \bar{C} e^{-i\alpha_2 x} + \bar{D} e^{i\alpha_2 x}. \quad (49)$$

Rearranging this solution leads to the general solution of equation (43) (see Bottega [22]):

$$\bar{y} = A \sinh \alpha_1 x + B \cosh \alpha_1 x + C \sin \alpha_2 x + D \cos \alpha_2 x. \quad (50)$$

Applying the boundary conditions results in the characteristic equation from which the natural frequencies can be found:

$$\omega[\tilde{m}(\alpha_2^3 \coth(\alpha_1 l) - \alpha_1^3 \tan(\alpha_2 l)) + \tilde{M}\omega\beta] = 0. \quad (51)$$

The solution of the characteristic equation (51) yields the set of the natural frequencies of the system ω_n with $n = 1, 2, \dots, \infty$. By observation it can be seen that the first natural frequency of the system equals zero, i.e., $\omega_1 = 0$, which implies rigid body motion. The mode associated with this natural frequency is found by substituting $\omega = 0$ into equation (43), which results in the partial differential equation for the rigid body motion,

$$\bar{y}_{xxxx} + N\bar{y}_{xx} = 0, \quad (52)$$

with the boundary conditions

$$\text{at } x = 0 \quad \begin{cases} \bar{y} = 0, \\ \bar{y}_{xx} = 0; \end{cases} \quad \text{at } x = l \quad \begin{cases} \bar{y}_{xx} = 0, \\ \bar{y}_{xxx} + N\bar{y}_x + \tilde{M}\Omega^2\bar{y} = 0, \end{cases} \quad (53)$$

where Ω is the rigid body natural frequency.

The general solution of equation (52) is

$$\bar{y} = A_1 + A_2 x + A_3 \sin \sqrt{N}x + A_4 \cos \sqrt{N}x, \quad (54)$$

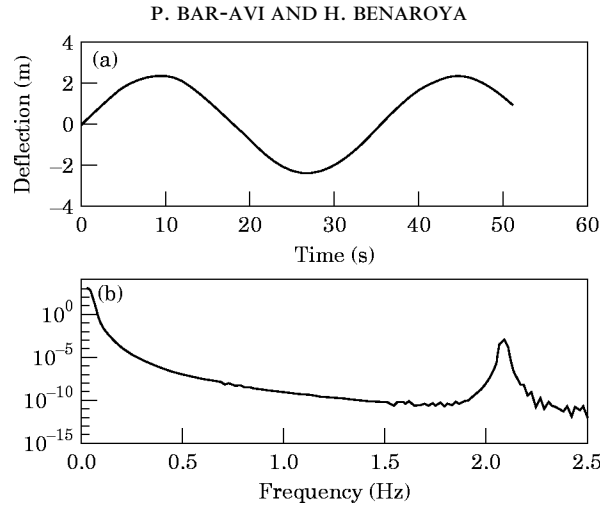


Figure 5. Free vibration in (a) the time domain and (b) the frequency domain.

which consists of a rigid body motion and an elastic motion. Applying the boundary conditions leads to

$$y = A_2 x \sin \Omega t, \quad (55)$$

where Ω is the natural frequency of the rigid body, given by

$$\Omega^2 = g(\frac{1}{4}\rho\pi D^2 d - M)/ML. \quad (56)$$

This solution agrees with the one found in the paper by Bar-Avi and Benaroya [1]. The first two natural frequencies and modes of the system are shown in Figure 5. Two frequencies can be seen. The low natural frequency is the rigid body frequency $\Omega = 0.028$ Hz. The high natural frequency is the first elastic frequency, $\omega_1 = 2.1$ Hz, which agrees with the semi-analytical solution. Also, the figure shows that the rigid body mode is of a much higher amplitude than the elastic mode. In fact the ratio between the

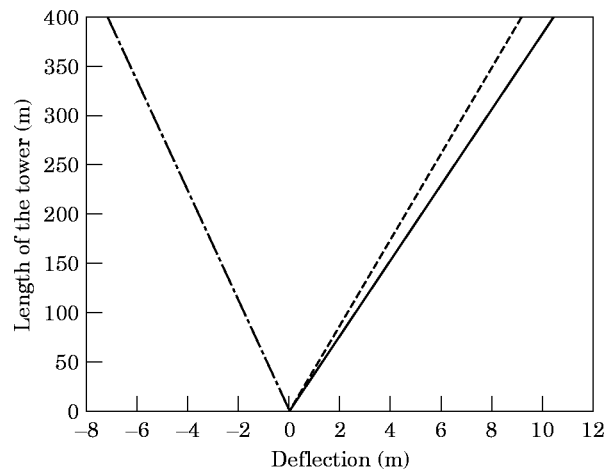


Figure 6. The response of the tower to wave excitation at different times: \cdots , $t = 25$ s; --- , $t = 50$ s; --- , $t = 100$ s.

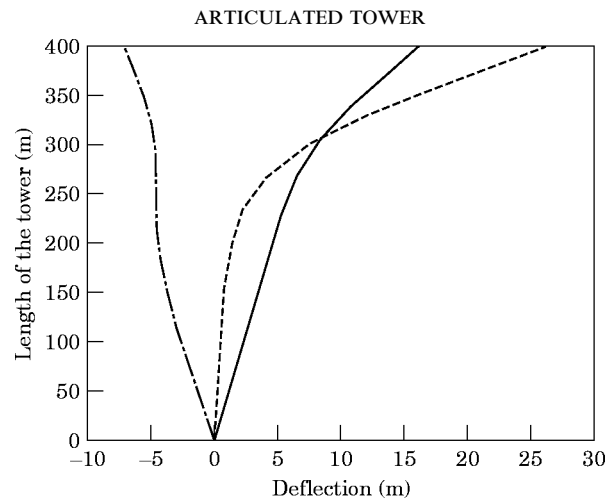


Figure 7. The response of the flexible tower to wave excitation at different times: - · - · - , $t = 25$ s; — , $t = 50$ s; - - - , $t = 100$ s.

amplitudes is about $A(\Omega)/A(\omega_1) \simeq 1000$, which means that the elastic motion is negligible from the point of view of structural dynamics.

The tower's response to wave excitation at different times— $t = 25, 50$ and 100 s is shown in Figure 6. It is seen that the response is as a rigid body because the deflection y changes linearly with its length x , as predicted in the semi-analytical solution.

When the diameter of the tower was changed to $D = 1.9$ m such that the first elastic natural frequency was $\omega_1 = 0.035$ Hz, the response to the same wave excitation is totally different, as depicted in Figure 7. The tower's response is no longer as a rigid body, since its first elastic natural frequency is very close to not only the rigid body natural frequency, but also to the wave excitation frequency.

7.2. RESPONSE OF AN APPENDAGED TOWER

In this section the response of an appendaged tower, such as an antenna or a mast connected to the deck of an articulated tower, is investigated. It is assumed that the inertia

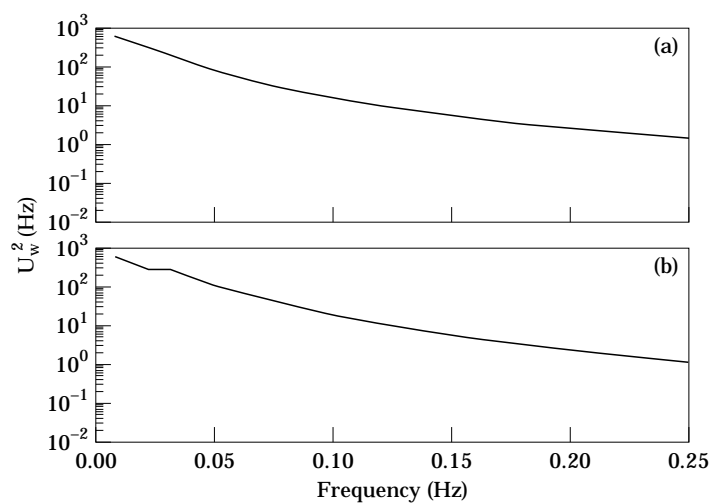


Figure 8. A comparison between (a) the actual Davenport spectrum and (b) the approximated spectrum.

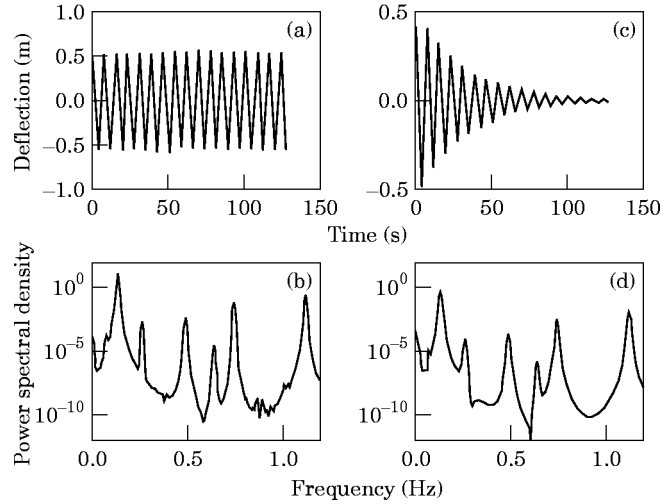


Figure 9. The free vibration response in the time and frequency domain: (a, b) without damping; (c, d) with structural damping. $\zeta = 0.04$.

of the mast is very small compared to the articulated tower to which it is connected. Hence, the mast has no effect on the tower. The mast is fixed at the bottom and has a concentrated mass at its top. It is subjected to deterministic and random wind loads as well as horizontal and vertical base excitation. These motions are derived from the response of the articulated tower that was investigated in Bar-Avi and Benaroya [1]. The following physical parameters are used in the analysis: the mast length, $l = 35$ m; the mast's diameter is tapered, $D = 0.3$ m at the bottom, to 0.2 m at the top; Young's modulus, $E = 2.04 \times 10^{11}$ N/m²; the mast density, $\rho_T = 7800$ kg/m³; the end mass, $M = 250$ kg; the deterministic wind mean speed at 10 m, $U_{10} = 10$ – 20 m/s; the gust wind mean speed at 10 m, $U_{gust} = 15$ m/s; the wind drag coefficient, $C_{D_a} = 1.4$.

The analysis includes free vibration, the response due to base excitation, the response due to deterministic and random wind speed, and the combination of both. Many types of random wind speed spectra exist in the literature. Among them are spectra due to

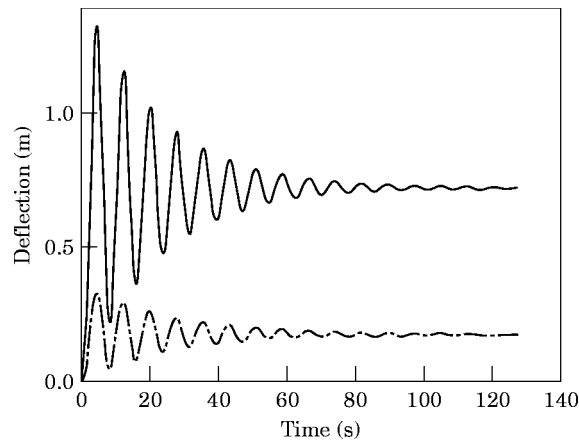


Figure 10. The equilibrium position in the presence of wind: —, $U_{10} = 20$ m/s; - · -, $U_{10} = 10$ m/s.

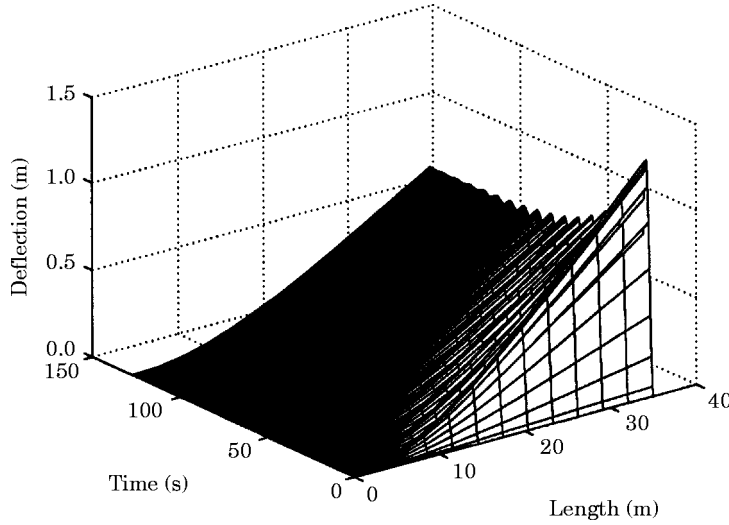


Figure 11. The equilibrium position of the whole mast due to a wind speed of $U_{10} = 20$ m/s.

Davenport, Harris, Kareem and others; see Chakrabarti [26, p. 101]. In the investigation presented here, the Davenport spectrum is assumed (Patel [24, p. 187]),

$$S_{vv}(f) = \frac{4k\bar{f}}{(1 + \bar{f}^2)^{4/3}} \frac{U_{gust}^2}{f}, \quad (57)$$

where f is the loading frequency in Hz, U_{gust} is the mean gust wind velocity, k is the sea surface drag coefficient (taken to be 0.005), and \bar{f} is a normalized frequency, given by

$$\bar{f} = fL/U_{gust}, \quad (58)$$

with L being a representative length scale, taken to be 1200 m.

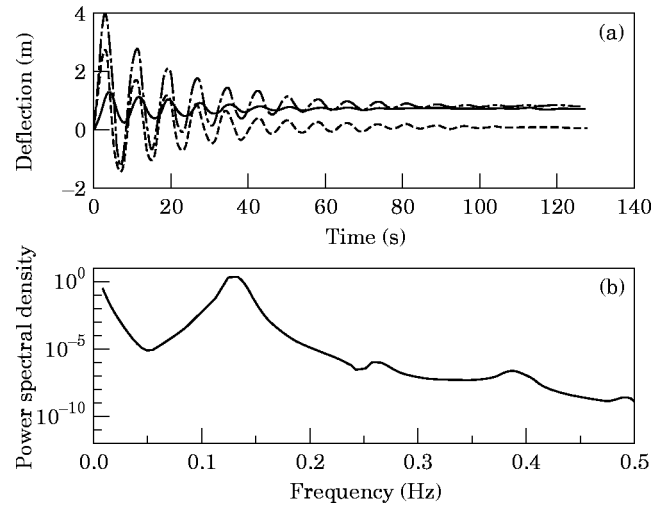


Figure 12. The response to wind force excitation in (a) the time and (b) the frequency domain: —, $U_{10} = 20$ m/s; ---, $U_{gust} = 15$ m/s; - · - · -, both.

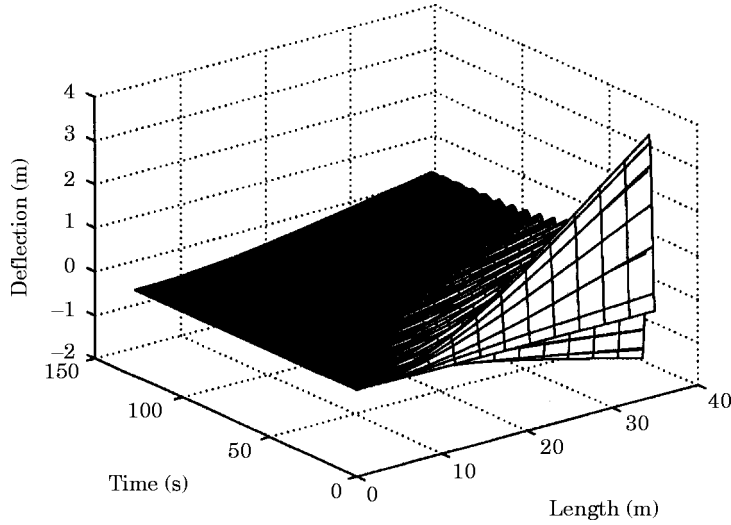


Figure 13. The mast's response to deterministic and random wind excitation.

To solve the equation numerically, the wind speed spectrum had to be transformed from the frequency domain into the time domain. Borgman's method was used to transform the Pierson–Moskowitz spectrum, but could not be utilized here due to a major difference between the Pierson–Moskowitz spectrum and the Davenport spectrum. Hence a brute force approximation is used. The spectrum is approximated as a series of sine functions with amplitudes that are calculated from equation (57),

$$U_w(t) = \sum_{i=1}^n A_i \sin(f_i t), \quad (59)$$

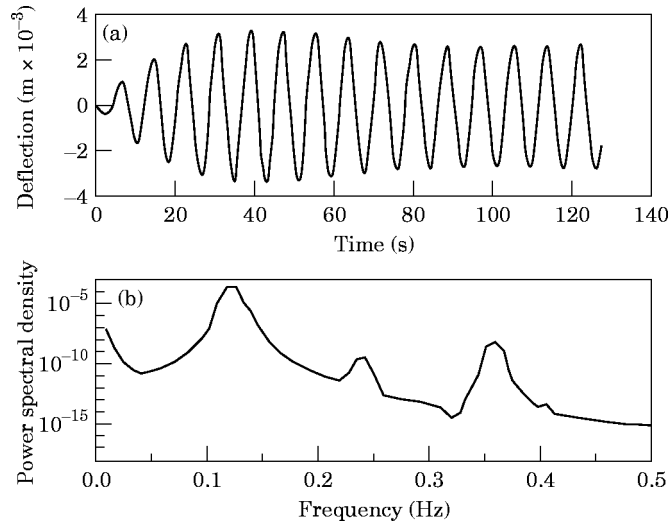


Figure 14. The (a) time and (b) frequency domain responses of the top end of the mast due to deterministic wave height.

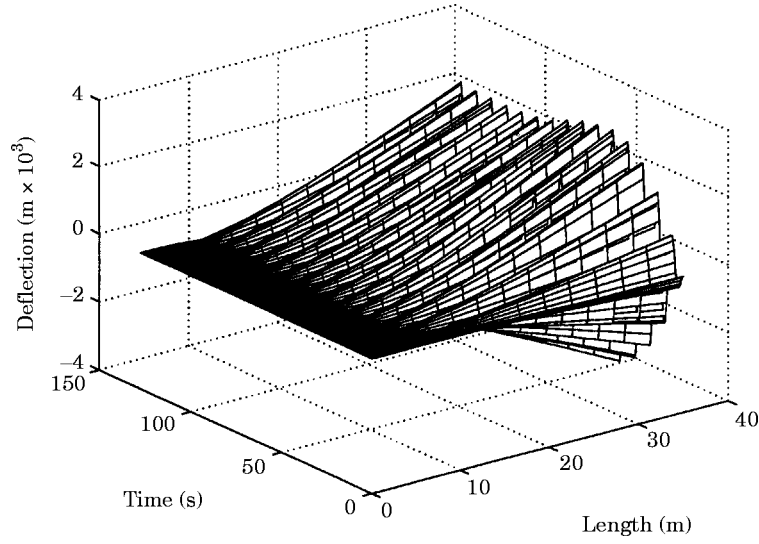


Figure 15. The response of the whole mast to deterministic wave excitation.

where

$$A_i = 2U_{gust} \sqrt{\frac{kf_i}{(1 + f_i^2)^{4/3}}}, \tag{60}$$

where n is the number of divisions of the frequency span. The actual Davenport spectrum and the approximated one are shown in Figure 8. As can be seen, they agree quite well. It should be noted that equations (59) and (60) result in a single realization of the random wind velocity. There is no randomness *per se*, but the input is representative of a random wind. Therefore, the response is one realization of all possible random forces.

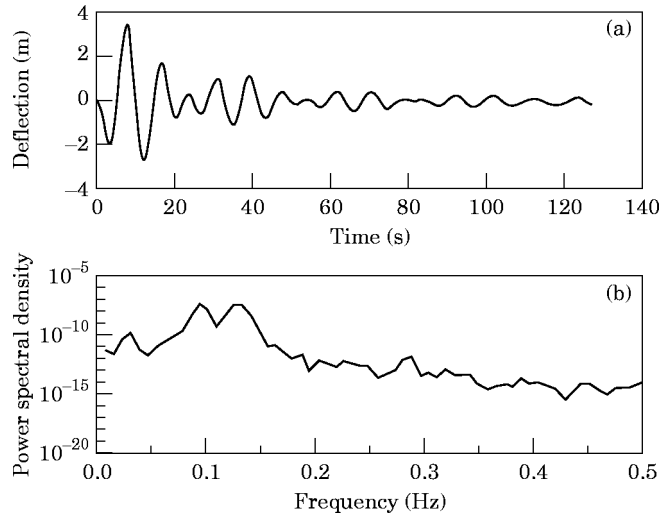


Figure 16. The (a) time and (b) frequency domain responses of the top end of the mast due to random wave height.

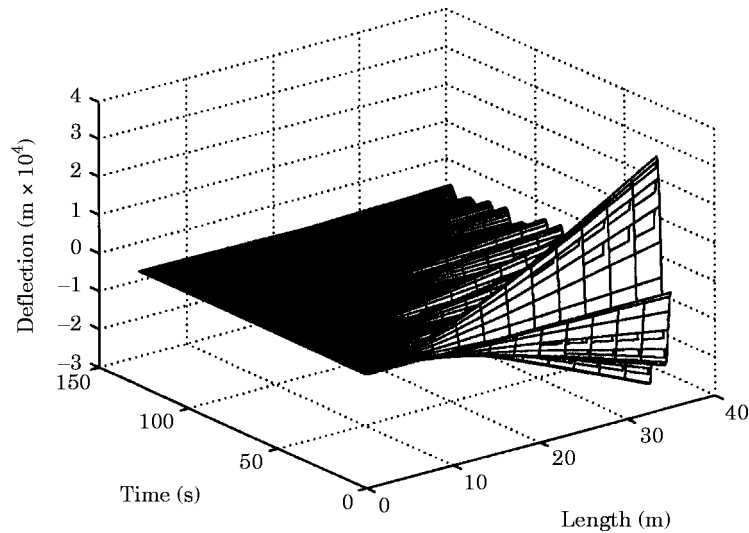


Figure 17. The response of the whole mast to random wave excitation.

First, the natural frequencies of the mast are found from the free vibration response depicted in Figure 9. The figure shows the response of the top end of the mast in time and frequency domains, with structural damping, $\zeta = 0.04$ (Figures 9(c) and (d)), and without damping (Figures 9(a) and (b)). The first peak corresponds to the first fundamental frequency, $\omega_1 = 0.13$ Hz, and the highest peak corresponds to the second fundamental frequency, $\omega_2 = 1.12$ Hz. The peaks in between are multiples of the first natural frequency resulting from the non-linearity of the system. From a linear eigenvalue analysis performed by “ACSL”, the same two fundamental frequencies were found.

Constant wind causes the mast to change its equilibrium position, just as the current does to the articulated tower. Since the wind force is proportional to the square of the wind speed, the mast's equilibrium position is also proportional to the square of the wind speed. The motion of the mast's top end when exposed to wind speeds of $U_{10} = 10$ m/s and $U_{10} = 20$ m/s is described in Figure 10. It is clearly seen that the response due to a

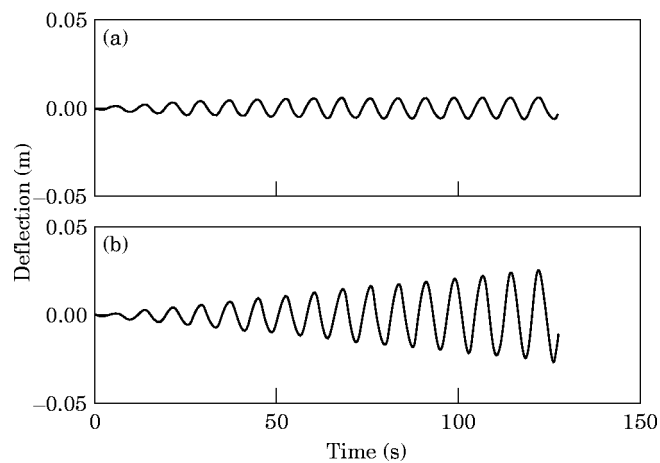


Figure 18. Parametric instability due to vertical base excitation in the natural frequency: (a) with structural damping, $\zeta = 0.04$; (b) no damping.

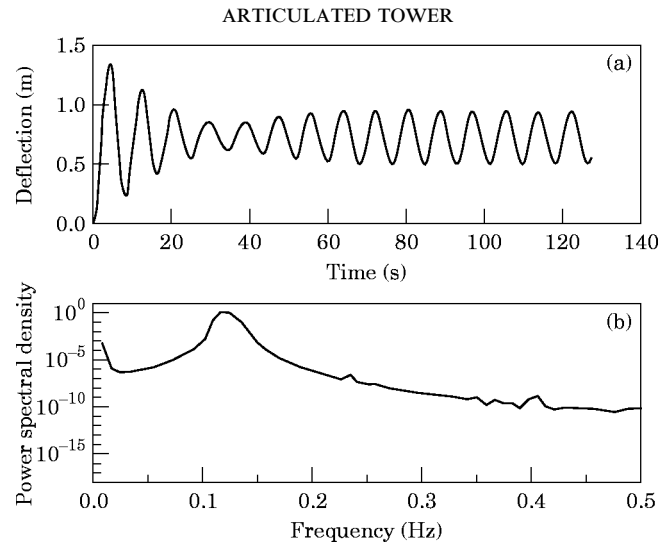


Figure 19. The (a) time and (b) frequency domain responses of the top end of the mast due to deterministic waves and wind excitation.

wind speed of 20 m/s (solid line) is four times larger than the one for a wind speed of 10 m/s (dashed line). The response of the whole mast to a wind speed of 20 m/s is depicted in Figure 11.

The response of the mast's top end to constant wind speed, random wind speed and a combination of both, is depicted in Figure 12. The solid line is the mast's response for deterministic wind speed of 20 m/s. The dashed line is for random wind speed having a mean speed of 15 m/s, and the dashed solid line is the response due to both. The first natural frequency of the mast is clearly seen from the response in the frequency domain. The response of the whole mast due to both random and deterministic wind speed is described in Figure 13.

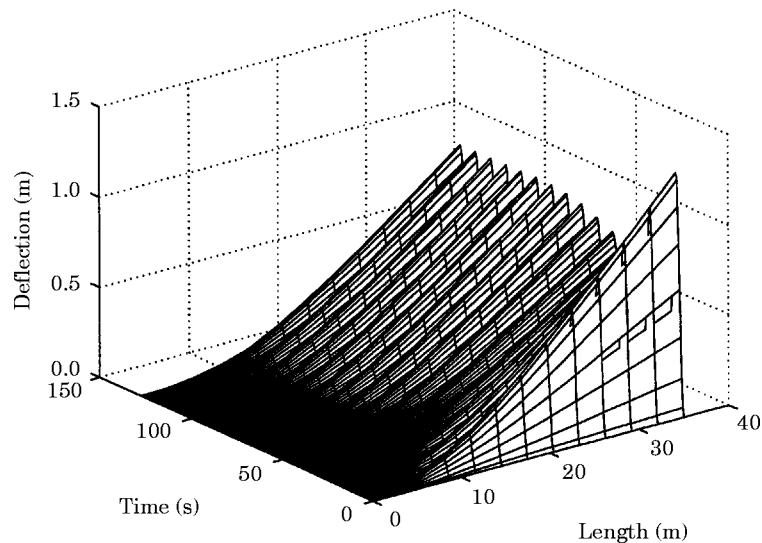


Figure 20. The response of the whole mast to deterministic waves and wind excitation.

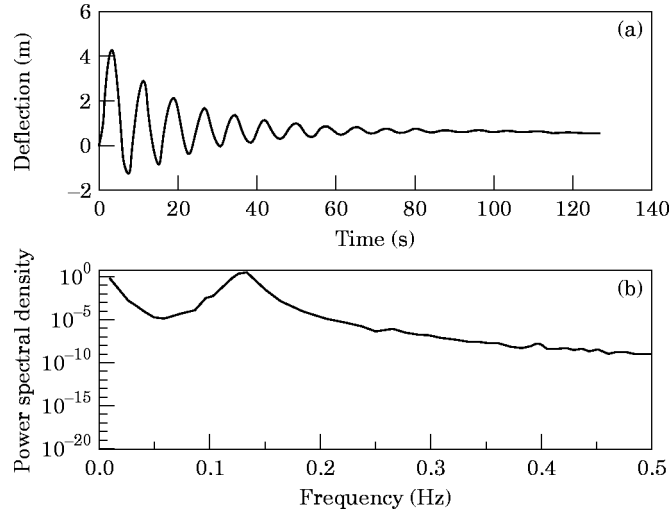


Figure 21. The (a) time and (b) frequency domain responses of the top end of the mast due to random waves and wind excitation.

The response of the mast due to the motion of the articulated tower is investigated next. As mentioned earlier, the base excitation is derived from the solution of the partially submerged articulated tower [1]. From the deflection angle $\theta(t)$ of the articulated tower due to waves, the horizontal u and vertical w base motions are found:

$$w = 400 \sin \theta(t), \quad u = 400(1 - \cos \theta(t)). \quad (61)$$

The horizontal motion u and its time derivatives have the same effect on the mast as an external force, while the vertical base excitation w and its derivative are part of the equation of motion and for certain amplitude and frequency can cause parametric instability, as will be shown later.

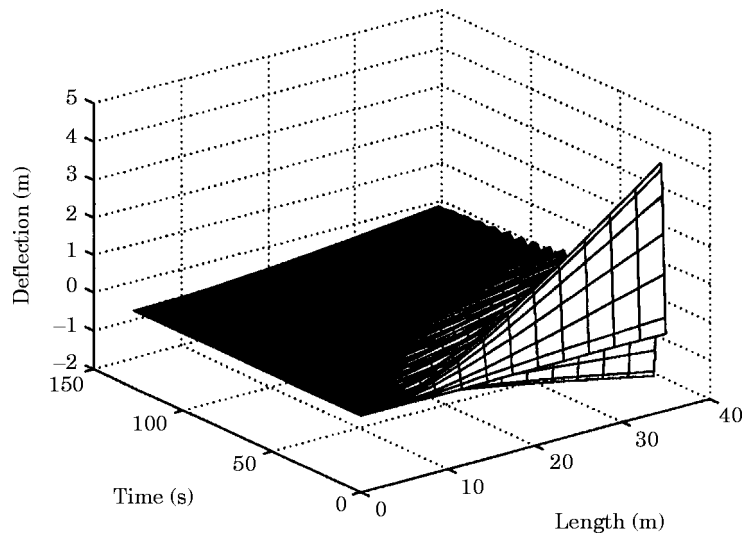


Figure 22. The response of the whole mast to random waves and wind excitation.

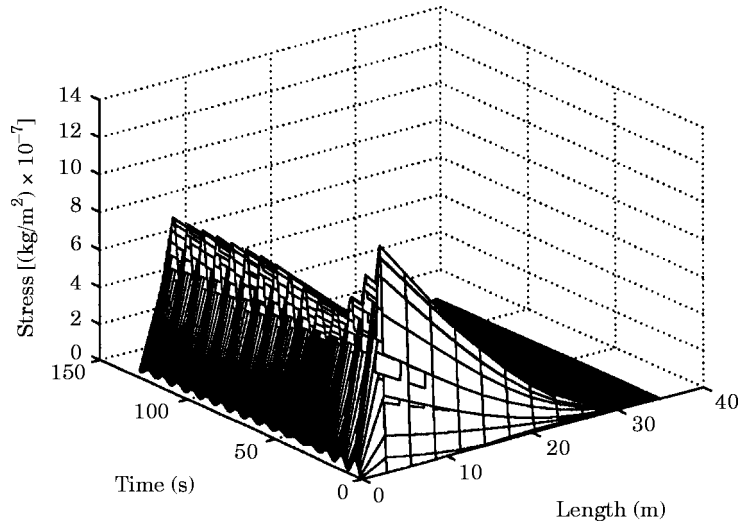


Figure 23. The equivalent stress due to deterministic waves and wind.

The response to deterministic wave excitation having a height of $H = 3$ m and frequency $\omega = 0.12$ Hz is shown in Figure 14. The time domain response of the top end of the mast is seen to beat because the excitation frequency is very close to the first natural frequency of the system, $\omega_1 = 0.128$ Hz. The response of the whole mast is depicted in Figure 15.

The motion of the top end of the mast to random wave excitation having a significant height of $H_s = 4$ m is shown in Figure 16, and Figure 17 shows the response of the whole mast. Because the excitation frequency of the deterministic wave is very close to first natural frequency of the mast, the response to deterministic waves has higher amplitudes than the random response.

When the frequency of the base excitation coincides with the first natural frequency of the mast, instability occurs, as can be seen from Figure 18. In the absence of damping a

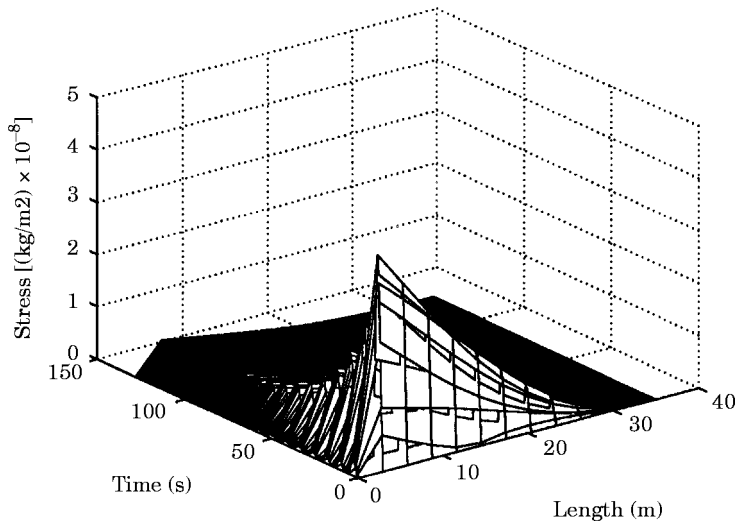


Figure 24. The equivalent stress due to random waves and wind.

very low amplitude can cause instability, but when damping is added to the system a larger amplitude is needed to cause instability.

The dynamic response of the mast to wind and wave excitation is shown next. The response of the mast due to deterministic wave and wind excitation is depicted in Figures 19 and 20. The wind speed is set to $U_{10} = 20$ m/s and the waves have the same parameters as in Figure 14. In Figure 19 are shown the time and frequency domain responses of the top end of the mast, and in Figure 20 is shown the response of the whole mast.

The response of the mast to random waves and wind is depicted in the following two figures. In Figure 21 is shown the top end motion and in Figure 22 is shown the response of the whole mast. The wind speed is $U_{gust} = 15$ m/s and the significant wave height is set to $H_s = 4$.

By comparing the results of the responses due to wind and wave to those due only to wind, it can be seen that the base excitation response is negligible compared to that due to the wind. It plays an important role only when parametric instability occurs.

The equivalent stress due to deterministic waves and wind excitation (same parameters as in Figure 19) is depicted in Figure 23, and the stresses due to random waves and wind (same parameters as in Figure 21) are shown in Figure 24.

Although this section is primarily an exercise, it demonstrates how the modes developed herein can be utilized in a risk and reliability framework. Cycles can be counted, and exceedances of certain stress levels can also be added for a measure of damage accumulation.

8. SUMMARY

The non-linear partial differential equation of motion for a tower having a concentrated mass at the top has been derived. The tower is modelled as a continuous system; that is, a beam-like structure, subjected to wave, wind and base excitation motions. The general non-linear partial differential equation of motion is derived using Hamilton's principle. All forces are determined at the instantaneous position of the tower, and expressed in a fixed co-ordinate system, causing the equation of motion to be highly non-linear. The equation is then non-dimensionalized and rotational terms are shown to be negligible. Expressions for the axial and shear stresses are also found.

The articulated tower discussed in Bar-Avi and Benaroya [9] as a rigid body is analyzed as an elastic body; that is, assuming that it has a finite rigidity. The governing partial differential equation of motion is simplified and then a semi-analytical solution is obtained using separation of variables. From the solution it is found that the structure's motion has two components, a rigid body motion and an elastic motion, as expected. The rigid body motion has a very low frequency, $\Omega = 0.028$ Hz, compared to the first elastic natural frequency $\omega_1 = 2.11$ Hz. Furthermore, the ratio between the amplitude of the first elastic mode to the amplitude of the rigid body mode is found to be $A(\omega_1)/A(\Omega) \simeq 1/1000$, which means that the elastic motion is negligible from the point of view of structural dynamics. The rigid body solution is found to be

$$y = Ax \sin \Omega t, \quad (62)$$

which is confirmed by a numerical solution obtained using "ACSL". From this analysis it is concluded that the rigid body assumption used for these kinds of structures is valid.

The response of a mast connected to the deck of an offshore articulated tower is then investigated. In this analysis the mast is assumed to be fixed to the bottom and carrying

a concentrated mass at the top. The mast is subjected to deterministic and random wind forces, as well as to base excitation.

First, the equilibrium position due to wind is found. Wind forces are similar to current forces and they cause the mast to deflect to a stationary equilibrium position. The deflection of the mast is proportional to the air drag coefficient and to the square of the wind speed.

To find the response due to random wind velocity, the Davenport spectrum is used. First, the spectrum is transformed into a time history function, which is essentially a sum of sine functions, with varying amplitudes and frequencies. The response to random wind velocity with gusting mean speed $U_{gust} = 15$ m/s is larger than for a deterministic wind speed with mean velocity $U_{10} = 20$ m/s.

The base excitation has a horizontal component that acts like an external force, and a vertical one that acts as a parametric excitation. Although the response of the mast to base excitation is very small compared to the response due to wind, it is very important because, for certain parameters, i.e., frequency and amplitude, it can cause instability.

Finally, the stresses along the mast are evaluated, and it is found that a combination of deterministic wind speed $U_{10} = 20$ m/s and random wind speed with a mean gust $U_{gust} = 15$ m/s results in a maximum equivalent stresses $\sigma_{eq} = 1.5 \times 10^8$ N/m² at the base of the mast. The yield stress of steel bar in tension is $\sigma_y = 2.8 \times 10^8$ N/m². It is concluded that wind forces are very important in analyzing these kinds of structures.

REFERENCES

1. P. BAR-AVI and H. BENAROYA 1996 *Journal of Sound and Vibration* **190**, 77–103. Non-linear dynamics of an articulated tower submerged in the ocean.
2. S. K. CHAKRABARTI and D. C. COTTER 1979 *Journal of the Waterway, Port, Coastal and Ocean Division, American Society of Civil Engineers* **105**, 281–292. Motion analysis of articulated tower.
3. O. GOTTLIEB, C. S. YIM and R. T. HUDSPETH 1992 *International Journal of Offshore and Polar Engineering* **2**(1), 61–66. Analysis of non-linear response of an articulated tower.
4. P. K. MUHURI and A. S. GUPTA 1983 *Ocean Engineering* **10**(6), 471–479. Stochastic stability of tethered buoyant platforms.
5. K. JAIN and T. K. DATTA 1987 in *Deep Offshore Technology, 4th International Conference and Exhibit*, 191–208. Stochastic response of articulated towers.
6. T. K. DATTA and A. K. JAIN 1990 *Computers and Structures* **34**, 137–144. Response of articulated tower platforms to random wind and wave forces.
7. A. K. JAIN and T. K. DATTA 1991 *Journal of Engineering for Industry* **113**, 238–240. Non-linear behavior of articulated tower in random sea.
8. P. BAR-AVI and H. BENAROYA 1995 *Accepted for publication in International Journal of Nonlinear Mechanics*. Response of a two DOF articulated tower to different environmental conditions.
9. P. BAR-AVI and H. BENAROYA 1995 *Accepted for publication in International Journal of Nonlinear Mechanics*. Stochastic response of an articulated tower.
10. C. L. KIRK and R. K. JAIN 1977 in *The 9th Annual Offshore Technology Conference*, 545–552. Response of articulated tower to waves and current.
11. R. K. JAIN and C. L. KIRK 1981 *Journal of Energy Resources Technology* **103**, 41–47. Dynamic response of a double articulated offshore loading structure to noncollinear waves and current.
12. O. A. OLSEN, A. BRAATHEN and A. E. LOKEN 1978 *Norwegian Marine Research*, **2**, 14–28. Slow and high frequency motions and loads of articulated single point mooring system for large tanker.
13. S. K. CHAKRABARTI and D. C. COTTER 1980 *Journal of the Waterway, Port, Coastal and Ocean Division, American Society of Civil Engineers* **107**, 65–77. Transverse motion of articulated tower.
14. R. ADREZIN, P. BAR-AVI and H. BENAROYA *Accepted for publication in ASCE Journal of Aerospace Engineering*. Dynamic response of articulated towers.

15. K. F. HAVERTY, J. F. MCNAMARA and B. MORAN 1982 in *Proceedings of the International Conference of Marine Research Ship Technology and Ocean Engineering*, 145–157. Finite dynamics motions of articulated offshore loading towers.
16. J. F. MCNAMARA and M. LANE 1984 *Journal of Energy Resources Technology*, 444–450. Practical modeling for articulated risers and loading columns.
17. J. W. LEONARD and R. A. YOUNG 1985 *Engineering Structures* **7**, 74–84. Coupled response of compliant offshore platforms.
18. G. SEBASTIANI, R. BRANDI, F. D. LENA and A. NISTA 1984 in *The 16th Annual Offshore Technology Conference*, 379–388. Highly compliant column for tanker mooring and oil production in 100 m water depth.
19. A. W. DARE 1967 *Schaum's Outline of Theory and Problems of Lagrangian Dynamics*. New York: McGraw-Hill.
20. R. COURANT and D. HILBERT 1962 *Methods of Mathematical Physics*. New York: John Wiley.
21. P. BAR-AVI and I. PORAT 1994 *The International Journal of Mechanical Engineering Education* **23**, 215–228. A sound derivation of the nonlinear equations of motion of a traveling string.
22. W. J. BOTTEGA 1986 *Dynamics and Stability of Systems* **1**, 201–215. Dynamics and stability of support excited beam-column with end mass.
23. O. M. FALTINSEN 1994 *Sea Loads on Ships and Offshore Structures*. Cambridge: Cambridge University Press.
24. M. H. PATEL 1988 *Dynamics of Offshore Structures*. London: Butterworth.
25. E. MITCHELL 1994 Solving PDES in ACSL by discretization and conversion to ordinary differential equations. Mitchell and Gauthier Associates, Technical Report 1–16.
26. S. K. CHAKRABARTI 1990 *Nonlinear Methods in Off-shore Engineering*. Amsterdam: Elsevier.